Defect-related versus excitonic visible light emission from ion beam synthesized Si nanocrystals in SiO_2

K. S. Min,[a] K. V. Shcheglov, C. M. Yang, and Harry A. Atwater
Thomas J. Watson Laboratory of Applied Physics, California Institute of Technology, Pasadena, California 91125

M. L. Brongersma and A. Polman
FOM Institute for Atomic and Molecular Physics, Kruislaan 407, 1098 SJ Amsterdam, the Netherlands

(Received 3 July 1996; accepted for publication 18 July 1996)

Two sources of room temperature visible luminescence are identified from SiO_2 films containing ion beam synthesized Si nanocrystals. From a comparison of luminescence spectra and photoluminescence decay lifetime measurements between Xe^+-implanted SiO_2 films and SiO_2 films containing Si nanocrystals, a luminescence feature attributable to defects in the SiO_2 matrix is unambiguously identified. Hydrogen passivation of the films selectively quenches the matrix defect luminescence, after which luminescence attributable to Si nanocrystals is evident, with a lifetime on the order of milliseconds. The peak energy of the remaining luminescence attributable to Si nanocrystals ''redshifts'' as a function of different processing parameters that might lead to increased nanocrystal size and the intensity is directly correlated to the formation of Si nanocrystals. Upon further annealing hydrogen-passivated samples at low temperatures (<500 °C), the intensity of nanocrystal luminescence increases by more than a factor of 10. © *1996 American Institute of Physics.* [S0003-6951(96)01940-7]

Visible light emission from low-dimensional group IV materials has received worldwide attention over the past few years, due to scientific and technological interest in development of silicon-based light emitters that could be monolithically integrated with advanced silicon microelectronics.[1] Since the discovery of porous Si,[2] many techniques have been developed to synthesize light emitting group IV nanocrystals.[3–8] Ion beam synthesis of group IV nanocrystals in thermal SiO_2 offers several technologically important advantages, including integrated circuit process compatibility and significant control over the nanocrystal size distribution, as well as chemical and mechanical stability. Although ion beam synthesis has been widely reported,[6–8] the origin of visible luminescence from ion beam synthesized Si nanocrystals has so far been unclear, primarily due to a lack of distinction between luminescence originating from matrix defects and luminescence originating from nanocrystals. It is well known[9–11] that defects in SiO_2 display luminescence at various energies including the visible range, so the interpretation of luminescence spectra without distinction of the contribution from defects can be very misleading.

In this letter, we provide experimental results on Si nanocrystals in SiO_2 made by ion implantation that clearly distinguishes visible photoluminescence (PL) originating from the nanocrystals from that which originates from matrix defects. From a comparison of PL spectra and lifetime measurements between Xe^+-implanted SiO_2 and SiO_2 films containing nanocrystals, a luminescence feature is clearly identified as arising from irradiation-damaged SiO_2. We demonstrate that subsequent hydrogen passivation of the films containing nanocrystals completely quenches the defect-related luminescence. The remaining PL band attributable to Si nanocrystals displays ''redshifts'' in peak energy as a function of processing parameters that might lead to increases in nanocrystal size, and the measured lifetimes are on the order of milliseconds. Upon further annealing hydrogen passivated samples at low temperatures, the intensity of the PL band originating from Si nanocrystals increases by as much as a factor of 10.

Wet thermal SiO_2 films, 100 nm thick, grown on lightly *p*-doped (100) Si wafers were implanted at room temperature with 50 keV $^{28}Si^+$ at doses of $1\times10^{16}/cm^2$, $2\times10^{16}/cm^2$, and $5\times10^{16}/cm^2$, corresponding to peak excess Si concentrations of 2, 4, and 10 at. % Si, respectively, as calculated using the TRIM code.[12] The samples were subsequently annealed in high vacuum at temperatures ranging between 400 and 1200 °C for a fixed time of 10 min or for times ranging between 10 and 320 min at a fixed temperature of 1000 °C. For selected samples, the presence of Si nanocrystals was verified by transmission electron microscopy. Si $2p$ core level x-ray photoelectron spectroscopy (XPS) was performed using a monochromated Al $K\alpha$ radiation at 1487 eV. A pure Gaussian deconvolution of the (100) Si $2p_{3/2}$ signal revealed a full width at half maximum $\Delta E_{FWHM}=0.72$ eV. All XPS spectra were corrected for any charging effects by fixing the adventitious C(1s) binding energy at 285 eV. For transmission electron microscopy (TEM) and XPS studies, all samples were thinned using HF so that the analyzed cross section lies at the peak of the implantation distribution. Hydrogen passivation experiments were performed by means of low energy (600 eV) deuterium implantation using a Kauffman ion source and the D dose was determined by elastic recoil spectrometry using a 2.0 MeV $^4He^{++}$ beam. (Deuterium was chosen instead of hydrogen in order to facilitate concentration determination.) All photoluminescence spectra were taken with 50 mW/mm^2 excitation using 457.9 nm Ar^+ laser radiation, detected using a grating spectrometer and the thermoelectrically cooled 256×1024 Si CCD array

[a]Electronic mail: ksmin@daedalus.caltech.edu

Downloaded¬03¬Apr¬2006¬to¬131.215.225.171.¬Redistribution¬subject¬to¬AIP¬license¬or¬copyright,¬see¬http://apl.aip.org/apl/copyright.jsp

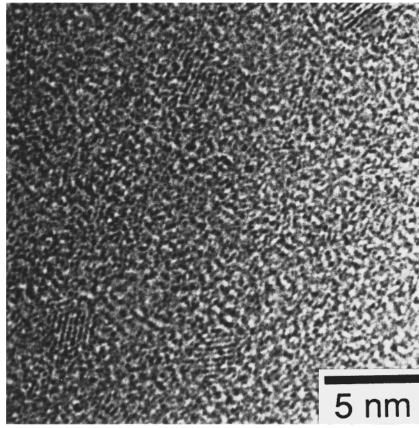

FIG. 1. High resolution TEM image of Si nanocrystals in SiO_2 synthesized from thermal SiO_2 implanted with 50 keV Si^+ to a dose of $5\times10^{16}/cm^2$. Precipitation was carried out by annealing in vacuum at 1000 °C for 40 min.

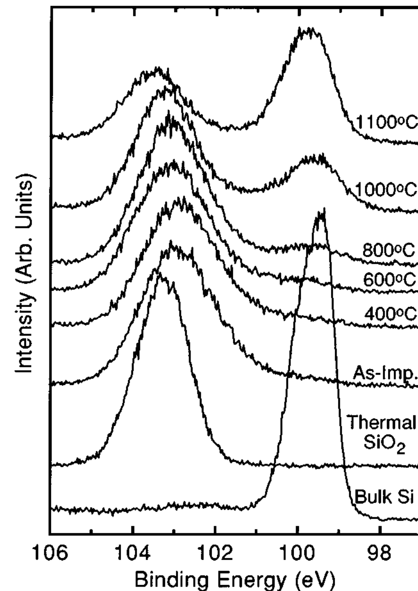

FIG. 2. XPS spectra of 50 keV Si^+-implanted SiO_2 ($5\times10^{16}/cm^2$ Si) annealed at various temperatures. As a comparison, XPS spectra of unimplanted 100 nm SiO_2 on Si and hydrogen terminated (100) bulk Si are also shown.

detector. All spectra have been corrected for system response. Samples for all PL lifetime measurements were cooled to 15 K using a closed-cycle He cryostat and pumped to a steady state with 475 nm Ar^+ laser radiation (1 mW/mm^2) prior to measurements. Lifetime traces were taken using a GaAs photomultiplier tube in combination with a multichannel photon counter. The time resolution of the experimental setup was 100 ns.

Figure 1 shows a plan-view high resolution TEM image of a SiO_2 film implanted with $5\times10^{16}/cm^2$ Si at 50 keV and annealed at 1000 °C for 40 min. Despite weak contrast, a dense array of Si nanocrystals is visible, with sizes ranging from 1 to 3 nm in diameter. It should be noted that due to low contrast between small Si nanocrystals and the amorphous SiO_2 background, quantitative information on size distribution of particles obtainable from TEM is limited and TEM analysis alone could lead to an underestimation of the particle density of small nanocrystals less than about 1.5 nm.

Additional information about nanocrystal formation was obtained using XPS. Figure 2 shows the Si $2p$ core level spectra of SiO_2 films implanted with $5\times10^{16}/cm^2$ Si and annealed at temperatures between 400 and 1100 °C for 10 min. For comparison, spectra of hydrogen terminated (100) Si and the unimplanted substrate (100 nm wet thermal SiO_2 on 100 Si) are also shown. Several trends are noteworthy in Fig. 2. First of all, the Si $2p$ core level of the as-implanted oxide film is shifted and inhomogeneously broadened towards lower binding energy relative to the unimplanted oxide, characteristic of a suboxide with contributions from various Si^{x+} oxidation states.[13] The phase separation of the suboxide into Si and SiO_2 occurs gradually with increasing annealing temperature, as can be deduced from the gradual shifting of the suboxide peak towards the stoichiometric SiO_2 binding energy and a distinct bulk Si peak appearing for samples annealed at temperatures higher than 600 °C. It is noteworthy that the presence of small nanocrystals for samples annealed at 800 and 600 °C can be inferred from the XPS spectra, although we could not observe them by transmission electron microscopy.

From the XPS spectra of Fig. 2, we can also obtain valuable information about the annealing kinetics of SiO_2, whose properties are known to be significantly altered during the process of ion implantation.[14] This is important for two reasons. First, suboxides leading to imperfect nanocrystal/SiO_2 interfaces could give rise to channels for nonradiative recombination of quantum-confined excitons. Second, it was previously demonstrated[11] from Xe^+-irradiated SiO_2 that some defects created during the implantation process display visible luminescence upon annealing at 800 °C. The analysis of Fig. 2 reveals that the peak of Si $2p$ core level of the damaged matrix approaches the value for stoichiometric SiO_2 only upon annealing at temperatures as high as 1100 °C. The full width at half-maximum, however, remains approximately 0.3 eV larger than that of the unimplanted film even after annealing at 1100 °C. We can, therefore, expect the presence of optically active defects in the damaged matrix even after high temperature annealing.

Figure 3(a) shows the PL spectra of the SiO_2 film implanted with 120 keV Xe^+ to a dose of $3\times10^{16}/cm^2$ and annealed at 1000 °C for 10 min. Upon annealing, the defect-related visible PL becomes intense, marked by a broad peak around 600 nm (2.07 eV) and a lifetime less than 100 ns at 550 nm (i.e., shorter than the experimental resolution of 100 ns). Figure 3(a) also illustrates that this defect-related visible PL can be completely quenched with about $3.3\times10^{15}/cm^2$ deuterium. Figure 3(b) illustrates the same set of experiments on SiO_2 films implanted with 50 keV Si^+. In addition to the defect-related PL band, the PL spectra of Si^+-implanted SiO_2 are characterized by the emergence of another PL band around 790 nm (1.57 eV) upon annealing at 1100 °C in vacuum for 10 min. While deuterium passivation leads to a complete suppression of the defect-related PL band around 600 nm, the intensity of the ''red'' PL band around 790 nm does not decrease further upon increasing the deuterium dose beyond $3.3\times10^{16}/cm^2$.

Several trends suggest that the origin of the ''red'' lumi-

Downloaded¬03¬Apr¬2006¬to¬131.215.225.171.¬Redistribution¬subject¬to¬AIP¬license¬or¬copyright,¬see¬http://apl.aip.org/apl/copyright.jsp

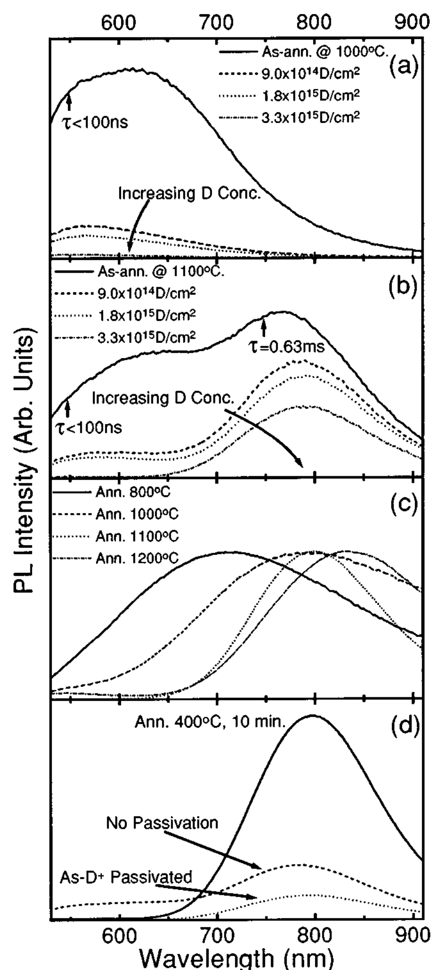

FIG. 3. Room temperature visible PL spectra and lifetime measurements of 100 nm SiO_2 films implanted with (a) 120 keV Xe^+ to a dose of $1.3 \times 10^{16}/cm^2$ and annealed at 1000 °C for 10 min and (b) 50 keV Si^+ to a dose of $5 \times 10^{16}/cm^2$ and annealed at 1100 °C for 10 min. Short arrows indicate the wavelengths at which lifetimes were measured. Long arrows indicate the effect of subsequent D passivation using 600 eV D; (c) PL peak energy shift of 50 keV Si^+-implanted SiO_2 after passivation. All samples were implanted with Si to a dose of $5 \times 10^{16}/cm^2$, annealed in vacuum, and subsequently passivated with $3.3 \times 10^{15}/cm^2$ D to quench the defect-related PL. All spectra are normalized; (d) PL intensity increase upon post-deuteration annealing the film of (b) at 400 °C for 10 min.

nescence can be attributed to radiative recombination of quantum-confined excitons. First, the value of the lifetime measured at 750 nm is consistent with theoretical predictions[15] for Si nanocrystals around 2.5 nm. In addition to a faster component limited by experimental resolution, a slower component was observed with a *1/e* decay time of 0.63 ms, as indicated in Fig. 3(b).

Second, the peak energy of the ''red'' luminescence after deuteration ''redshifts'' as a function of implantation dose and annealing temperature. This is illustrated in the normalized PL spectra of Fig. 3(c) for $5 \times 10^{16}/cm^2$ Si^+-implanted samples annealed at different temperatures. All samples were deuterated with an equal dose of deuterium of $3.3 \times 10^{15}/cm^2$. A clear shift in PL peak energy from 710 nm (1.75 eV) to 840 nm (1.48 eV) is observed between samples annealed at 800 and 1200 °C. Similarly, a shift from 650 nm (1.91 eV) to 790 nm (1.57 eV) was observed between samples implanted with $2 \times 10^{16}/cm^2$ Si and $5 \times 10^{16}/cm^2$ Si, respectively, after annealing at 1000 °C and passivating with $3.3 \times 10^{15}/cm^2$ deuterium.

Third, deuterated samples display a dramatic increase in PL intensity upon low temperature (<500 °C) post-deuteration annealing, which increases the mobility of deuterium atoms. It appears that the implanted deuterium atoms have enough mobility at room temperature to passivate defects in the matrix but require higher atomic mobility to further passivate dangling bonds at the nanocrystal/SiO_2 interface. This is illustrated in Fig. 3(d) for the deuterated sample of Fig. 3(b). Upon annealing at 400 °C for 10 min, the intensity of the ''red'' luminescence increases dramatically, by as much as a factor of 10. This is consistent with the notion that passivation of dangling bonds at the nanocrystal/SiO_2 interface leads to an enhancement of radiative recombination. The PL intensity increases to a maximum at post-deuteration annealing temperature of 400 °C and starts to decrease at higher temperatures, presumably due to the release of deuterium from defects at the nanocrystal/SiO_2 interface and subsequent out diffusion from the film.

Finally, the luminescence intensity scales with the volume density of Si–Si bonds, as revealed by XPS results. The luminescence intensity increases with increasing dose, annealing temperature, and annealing time. Increasing any one or more of these three processing parameters increases the intensity of bulk Si $2p$ core level signal in XPS, suggesting a corresponding increase in the volume density of Si–Si bonds. This is most likely associated with an increase in nanocrystal density, since the particles do not coarsen significantly beyond the size of about 2.5 nm, as deduced from our limited TEM results.

The authors acknowledge M. Easterbrook and A. Rice for technical assistance. This work was supported by the U.S. Department of Energy under Grant No. DE-FG03-89ER45395 and NATO Ministry for Scientific Affairs. The work at FOM was financially supported by NWO, STW, and IOP Electro-Optics.

[1] R. A. Soref, Proc. IEEE **81**, 1687 (1993).
[2] L. T. Cahnam, Appl. Phys. Lett. **57**, 1046 (1990).
[3] Y. Maeda, Phys. Rev. B **51**, 1658 (1994).
[4] Q. Zhang, S. C. Bayliss, and D. A. Hutt, Appl. Phys. Lett. **66**, 1977 (1995).
[5] L. E. Brus, P. F. Szajowski, W. L. Wilson, T. D. Harris, S. Schuppler, and P. H. Citrin, J. Am. Chem. Soc. **117**, 2915 (1995).
[6] T. S. Iwayama, S. Nakao, and K. Saitoh, Appl. Phys. Lett. **65**, 1814 (1994).
[7] P. Mutti *et al.*, Appl. Phys. Lett. **66**, 851 (1995).
[8] H. M. Cheong, W. Paul, S. P. Withrow, J. G. Zhu, J. D. Budai, C. W. White, and D. M. Hembree, Jr., Appl. Phys. Lett. **68**, 87 (1996); J. G. Zhu, C. W. White, J. D. Budai, S. P. Withrow, and Y. Chen, J. Appl. Phys. **78**, 4386 (1995).
[9] L. Skuja, J. Non-Cryst. Solids **179**, 51 (1994).
[10] K. S. Seol, A. Ieki, Y. Ohki, H. Nishikawa, and M. Tachimori, J. Appl. Phys. **79**, 412 (1996).
[11] K. S. Min, K. V. Shcheglov, C. M. Yang, H. A. Atwater, M. L. Brongersma, and A. Polman, Appl. Phys. Lett. **68**, 2511 (1996).
[12] J. F. Ziegler, J. P. Biersack, and U. Littmark, *The Stopping and Range of Ions in Solids* (Pergamon, New York, 1985).
[13] See, for example, Z. H. Lu, M. J. Graham, D. T. Jiang, and K. H. Tan, Appl. Phys. Lett. **63**, 2941 (1993).
[14] G. W. Arnold, J. Non-Cryst. Solids **179**, 288 (1994).
[15] M. Hybertsen, Phys. Rev. Lett. **72**, 1514 (1994).

Downloaded¬03¬Apr¬2006¬to¬131.215.225.171.¬Redistribution¬subject¬to¬AIP¬license¬or¬copyright,¬see¬http://apl.aip.org/apl/copyright.jsp